Characterization of a Dual-Excited Composite Transducer Comprising Central Mass With Equivalent Circuit

Igor Jovanović and Dragan Mančić

***Abstract*— The process of designing efficient ultrasonic transducers involves a detailed analysis of the transducer's mechanical and electrical characteristics for various operating conditions. If the transducer is radiating towards a complex acoustic load, the resonant frequency will change due to a change in the boundary condition on the working surface. In this paper, a simple model is proposed to improve the characterization process of a dual-excited composite transducer, by using an equivalent electromechanical circuit. The mentioned transducer is characterized by a middle mass which oscillates between two active piezoceramic stacks. The developed equivalent circuit was used to analyse the frequency response of the transducer incorporating the effects of varying the density and thickness of the central mass on the various characteristics of the transducer. The validity of the design was verified through the fabrication and characterization of few transducers.**

***Index Terms*— Composite Transducer; Equivalent Circuit Method; Input Electrical Impedance; Radiated Sound Pressure.**

I. Introduction

Technological application of a power ultrasound is extremely exploited in many branches of industry such as mining, ultrasonic machining, material processing, ultrasonic additive manufacturing, cutting, welding [1], ultrasonic extraction, sonochemistry, and other ultrasonic liquid processing applications where it is necessary to maintain a rapid flow of a liquid [2]. Ultrasound, without electromagnetic radiation [3], has been also widely used in the fields of fiber communication, Micro-electro-mechanical Systems, energy harvesting technologies [4, 5]. Non-flammable piezoelectric materials are increasingly being used as in piezoelectric transformers [6]. It is vital to design ultrasonic equipment that secures the required level of acoustic power in the radiating zone due to the range of uses for ultrasonic technologies. Still, some piezoelectric ultrasonic transducers do not have a high enough conversion efficiency of electrical energy into mechanical vibrations. The biggest disadvantage is the fact that only the acoustic characteristics of the load produce significant attenuation.

Igor Jovanović is with the University of Niš, Faculty of Electronic Engineering, 14 Aleksandra Medvedeva, 18000 Niš, Serbia (e-mail: igor.jovanovic@elfak.ni.ac.rs), ORCID ID (https://orcid.org/0000-0001-7912-9154).

Dragan Mančić is with the University of Niš, Faculty of Electronic Engineering, 14 Aleksandra Medvedeva, 18000 Niš, Serbia (e-mail: dragan.mancic@elfak.ni.ac.rs), ORCID ID (https://orcid.org/0000-0001-9713-8337).

That is why in this paper a structure of dual-excited ultrasonic transducer type, with lead zirconate titanate (PZT) piezoceramics, is proposed, because of its potential high-power, wide bandwidth characteristics and compact structure. The structure of dual-excited transducer is shown in the figure 1, and can be viewed as the vibration system of back mass (1) – PZT stack (PZT_{12}) – central-mass (2) - PZT stack (PZT_{34}) - front mass (3), the structure will generate two close resonant points. The PZT stacks couple with each other and generate two close harmonic frequencies, and then a needed bandwidth will be achieved in theory [7].

The acoustic performance of transducers is most often analysed by equivalent circuit method and finite element method [8]. A quick and effective way for examining a transducer's acoustic properties is the equivalent circuit method [9]. Namely, the basis of a large number of one-dimensional models (1D), including the equivalent circuit method, described in the literature for modelling, designing and optimizing ultrasonic transducers is Mason's model [10]. The equivalent circuit method is presented as a passive electromechanical equivalent circuit whose application is based on the idea that the propagation speed of ultrasonic waves is equivalent to electric current, while mechanical force is equivalent to electric voltage [11]. In the analysis using the mentioned method, the problems related to solving the system of wave equations in electromechanical systems can be overcome by applying the theory of electrical networks [12].

Therefore, this study proposes a new equivalent circuit approach to accommodate the mid mass element through its variable thickness and material properties. The analysis was performed through the curve of the change of resonance frequencies and sound pressure as a function of frequency.

II. Equivalent Electromechanical Equivalent Circuit of Composite Transducer

Fig. 1 depicts the 1D model of the transducer that accounts for the piezoelectric characteristics of the stimulating ceramic. The equivalent circuit model was created using 1D theory and updated in accordance with the literature's [13] description of the composite transducer's construction. In the provided 1D model, each transducer component's size, material properties, and resonance frequencies affect input electrical impedance.

Elements of the circuit shown in Fig. 1 corresponding to the isotropic metal transducer parts and the piezoceramic rings are calculated as:

 ISBN 978-86-7466-970-9

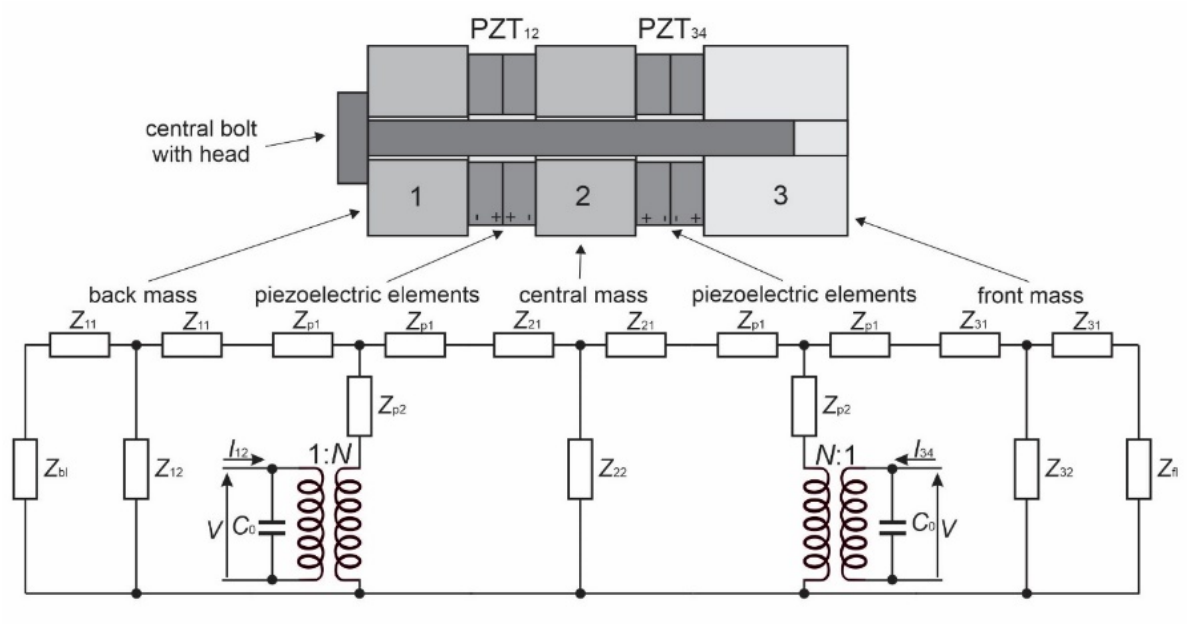

Fig. 1. Equivalent electromechanical circuit of composite transducer.

$$Z_{i1} = jZ_{ci}tg\frac{k_i l_i}{2},\ Z_{i2} = \frac{-jZ_{ci}}{\sin(k_i l_i)} \tag{1}$$

$$Z_{p1} = jZ_{cp}tg\frac{nk_p l_p}{2},\ Z_{p2} = \frac{-jZ_{cp}}{\sin(nk_p l_p)} \tag{2}$$

wherein $Z_{ci}=\rho_i v_i S_i$ are characteristic impedances and $k_i=\omega/v_i$ are corresponding wave numbers (for i=1, 2, 3). ρ_i are densities, l_i and S_i are lengths and surface areas of the cross-sections, v_i are the velocities of longitudinal ultrasonic waves propagation through the corresponding parts. In Eq. (2), the characteristic impedances and corresponding wave numbers are marked as $Z_{cp}=\rho_p v_p S_p$ and $k_p=\omega/v_p$, respectively. Densities, lengths, surface areas and velocities of longitudinal ultrasonic waves propagation of the piezoceramic cross-sections are ρ_p, l_p, S_p, and v_p, respectively. On Fig. 1, the input electric voltages and currents are marked as V, I_{12} and I_{34}.

The piezoceramics model consist of capacitance $C_0=n\varepsilon_{33}{}^S S_p/l_p$, and ideal transformers with transmission ratios $N=h_{33}C_0/n$, wherein n is the number of piezoceramic rings per the active layer (in the case of the particular composite transducers n is 2). The piezoelectric properties of the transducer active layers are represented by piezoelectric constant h_{33} and relative dielectric constant of the pressed ceramic $\varepsilon_{33}{}^S$.

Piezoceramic rings (between which is the central mass situated) are mechanically connected in series with back and front mass endings. Front mass and back mass are closed with acoustic impedances Z_{fl} and Z_{bl}, which are, in case of calculating input electrical impedance, negligible because experimental measurements were conducted with unloaded transducers oscillating in the air.

If the central bolt impact is neglected, based on the equivalent circuit scheme shown in Fig. 1, input electrical impedance can be calculated as:

$$Z_e = \frac{Z_{12}Z_{34}}{N^2\left(Z_{12}+Z_{34}\right)+j2\omega C_0 Z_{12}Z_{34}} \tag{3}$$

wherein $\omega=2\pi f$ is angular frequency, $Z_{12}=V/I_{12}$ and $Z_{34}=V/I_{34}$ are input electrical impedances of the corresponding active layers obtained by following expressions:

$$Z_{12} = \frac{Z_{e5}-\frac{Z_{e2}}{Z_{e3}}Z_{e6}}{Z_{e4}-\frac{Z_{e1}}{Z_{e3}}Z_{e6}},\ Z_{34} = \frac{Z_{e3}-\frac{Z_{e6}}{Z_{e5}}Z_{e2}}{Z_{e1}-\frac{Z_{e4}}{Z_{e5}}Z_{e2}} \tag{4}$$

In Eq. (4) the new equivalent impedances are acquired by following expressions:

$$Z_{e1} = 1+\frac{Z_{p1}+Z_{21}+Z_{22}}{Z_{e7}}+\frac{Z_{22}}{Z_{e8}},$$

$$Z_{e2} = Z_{22}+Z_{p2}+Z_{p1}+Z_{21}+\frac{Z_{p2}\left(Z_{22}+Z_{p1}+Z_{21}\right)}{Z_{e7}},$$

$$Z_{e3} = Z_{22}+\frac{Z_{p2}Z_{22}}{Z_{e8}}, \tag{5}$$

$$Z_{e4} = 1+\frac{Z_{p1}+Z_{21}+Z_{22}}{Z_{e8}}+\frac{Z_{22}}{Z_{e7}},$$

$$Z_{e5} = Z_{22}+\frac{Z_{p2}Z_{22}}{Z_{e7}},$$

$$Z_{e6} = Z_{22}+Z_{p2}+Z_{p1}+Z_{21}+\frac{Z_{p2}\left(Z_{22}+Z_{p1}+Z_{21}\right)}{Z_{e8}}.$$

 ISBN 978-86-7466-970-9

that is:

$$Z_{e7} = \frac{\left(Z_{bl} + Z_{11}\right) Z_{12}}{Z_{bl} + Z_{11} + Z_{12}} + Z_{11} + Z_{p1}, \quad (6)$$

$$Z_{e8} = \frac{\left(Z_{fl} + Z_{31}\right) Z_{e2}}{Z_{fl} + Z_{31} + Z_{32}} + Z_{31} + Z_{p1}, \quad (7)$$

Based on Eq. (3), expressions for resonant frequencies (f_r) can be derived as:

$$Z_{12} Z_{34} = 0 \quad (8)$$

Expressions for antiresonant frequencies (f_a) can be derived as:

$$N^2 \left(Z_{12} + Z_{34}\right) + j2\omega C_0 Z_{12} Z_{34} = 0 \quad (9)$$

The radiation impedance (Z_r) imposed on the front mass is given by Eq. (10). Assuming that the wavelength is much smaller than the transducer's radiating face, it can be assumed that in a large part of the observed frequency range, the thickness modes are the dominant vibration modes in the transducer, the whole system can be observed as a pure piston source. In this way, the radiation impedance can be approximately calculated as [14]:

$$Z_r = \rho_r v_r S_i \left[1 - \frac{J_1\left(2k_r r_i\right)}{k_r r_i} + \frac{jH_1\left(2k_r r_i\right)}{k_r r_i}\right] \quad (10)$$

wherein r_i and S_i are radius and surface areas of the cross-sections of metal endings (for pure piston, front mass is radiating metal ending so it is applied i=3), ρ_r, k_r and v_r are density, wave number and sound velocity of longitudinal ultrasonic waves propagation through the surrounding medium, respectively. J_1 and H_1 are first-order Bessel and Hankel functions.

When the PZT stacks, which are electrically coupled in parallel, are excited using a unit input voltage, the current flowing to the radiation impedance corresponds to the acoustic volume velocity. The total current flowing to the radiation impedance corresponds to the resultant volume velocity υ_r transmitted by the transducer.

The radiated sound pressure at a far-field distance r_d from the sound source can be expressed as [9]:

$$p = \sqrt{\frac{\left|\upsilon_r\right|^2 R_r \rho_r v_r}{4\pi r_d^2}} \quad (11)$$

wherein R_r is the radiation resistance, that is, it represents the real part of the radiation impedance Z_r in Eq. (10).

Thus, the approximate radiated sound pressure for the transducer can be calculated from Eq. (11) with the front mass velocity υ_r. The front mass velocity υ_r corresponds the current flowing to the radiation impedance Z_{fl} in the equivalent electromechanical circuit of composite transducer shown in the Fig. 1:

$$\upsilon_r = N \frac{U}{Z_{fl} + Z_{31}} \left(1 - \frac{Z_{p2}}{Z_{34}}\right)\left[1 - \frac{Z_{p1} + Z_{31}}{Z_{e8}}\right] \quad (12)$$

Due to the complexity of the expression of input electrical impedance for the whole composite transducer, the presented model of the composite transducer ignores the central bolt. The central bolt extends along the entire structure and if its influence is considered, it should be included in the model in such a way that it is connected mechanically in parallel to all elements in the scheme. Additionally, this model allows only the thickness resonant modes to be predicted and, therefore, do not take into the account the inevitable radial, and resonant modes other types.

III. Simulation and Experimental Results

Table 1 shows the dimensions of the realized composite transducers. Dimensions of the exciting piezoceramic rings are Ø38/Ø15/5 mm, and rings are made of PZT4 piezoceramic equivalent material [15]. l_i is the length, a_i and b_i are the outer and inner diameters of the corresponding i-th element. The front mass is made of dural, the back mass is made of steel, while the central mass is made of steel for transducers CT1-4 and is made of dural for transducer CT5, with the standard material properties.

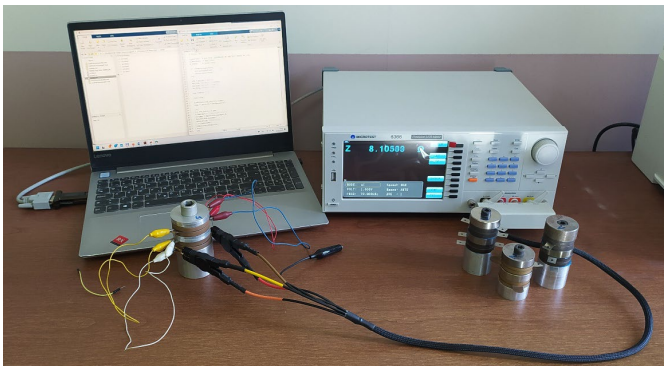

Fig. 2. Experimental set-up for the electrical impedance measurement.

The electrical impedance measurements are conducted using a Microtest 6366 Precision LCR Meter (Fig. 2). Figure 3 shows the change of resonance frequencies as a function of the central mass density. Simulated changes of f_r are marked with blue lines, while changes of f_a are marked with red lines, for the first two modes. The thickness of the front mass in the simulation was 17.5 mm, while the thickness ratios of the back and the central mass corresponded to: 10 mm/11 mm (solid lines), 11 mm/10 mm (dashed lines) and 10 mm/10 mm (dotted lines). Experimentally measured values are denoted with markers. The density of the central mass is chosen in the range from the density of magnesium 1740 kg/m^3, dural

 ISBN 978-86-7466-970-9

2800 kg/m^3, titanium 3700 kg/m^3, up to the density of steel 7850 kg/m^3.

TABLE I
DIMENSIONS OF COMPOSITE TRANSDUCERS USED IN EXPERIMENTAL ANALYSIS

	Composite transducers				
Dimension [mm]	**CT1**	**CT2**	**CT3**	**CT4**	**CT5**
l_1	10	11	10	11	11
l_2	11	10	10	11	11
l_3	18.5	17.5	18	16.5	18
$a_1=a_2=a_3$	40	40	40	40	40
$b_1=b_2$	9	9	9	9	9
b_3	8	8	8	8	8

It can be seen from Figure 3 that the density of the central mass has a great influence on the second resonant mode in such a way that with the increase in density the resonance frequencies of the second mode decrease. Also, the changes in the thickness of the back mass have a greater influence on the observed modes than the change in the thickness of the central mass, which is more noticeable in the case of the first resonant mode.

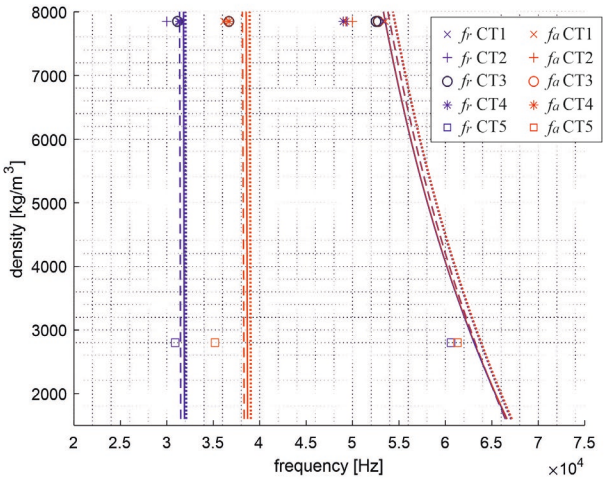

Fig. 3. Resonance frequencies change of the composite transducer, depending of the central mass density.

Figure 4 shows the change of resonance frequencies as a function of the thickness ratio of the central and back mass (dashed lines), as well as the thickness ratio of the central and front mass (solid lines). Simulated changes of f_r are marked with blue lines, while changes of f_a are denoted with red lines. Experimentally measured values are marked with markers. In this and all subsequent analyses, it is assumed that the central mass is made of steel, so the transducer CT5 is omitted.

In the observed transducers, the second mode is thickness, which means that the third mode (which is not thickness mode and is not included in the model) has a strong coupling with the second mode and affects its frequencies in a way that moves them to lower frequencies. Therefore, the measured frequencies of the second mode are significantly lower than the modeled frequencies.

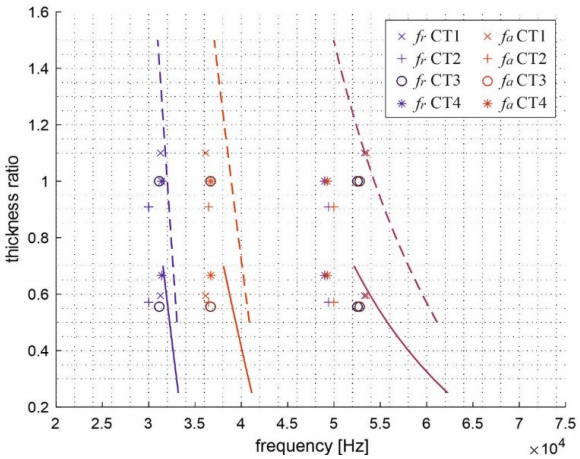

Fig. 4. Resonance frequencies change of the composite transducer depending on the thickness ratio of the central mass and the back mass (dashed lines), and the thickness ratio of the central mass and the front mass (solid lines).

Next analysis was performed through the curve of the change of sound pressure as a function of frequency. The approximate radiated sound pressure for the transducer can be calculated from Eq. (11), where the front mass velocity is calculated from the model shown in Fig. 1 using a 1 V drive signal. In the simulation, water with the following parameters was used as the transmission medium: density 1000 kg/m^3, sound velocity 1500 m/s, and far-field distance from the sound source is assumed to be 1 m.

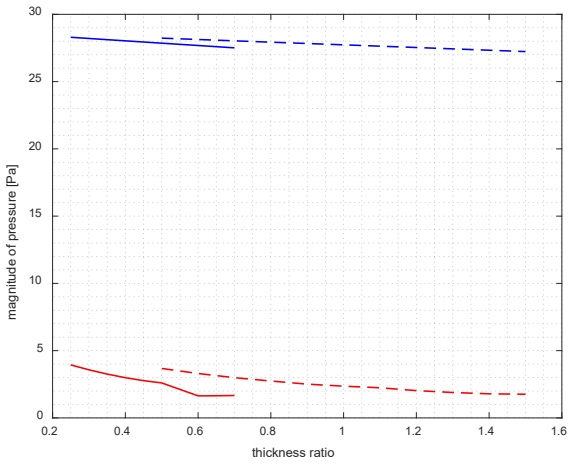

Fig. 5. Theoretical relationship between the sound pressure magnitude and the thickness ratio of the central mass and the back mass (dashed line), and the thickness ratio of the central mass and the front mass (solid line).

Figure 5 summarizes the effect of varying the thickness on the sound pressure magnitude p. Simulated changes of the pressure magnitude for first resonant mode are marked with blue lines, while changes for second resonant mode are denoted with red lines. The pressure magnitude gradually decreased as the central mass thickness increased. The decrease in the peak pressure magnitude was more prominent in the second mode. These results indicate that central mass element is more beneficial for enhancing second mode. This

 ISBN 978-86-7466-970-9

may be utilized to increase the bandwidth of dual-excited composite transducers.

IV. Conclusion

In this paper, an equivalent circuit was developed to represent the composite structure of the piezoelectric ultrasonic transducer, with the central mass sandwiched between two piezoceramic stacks. The equivalent circuit was used to analyze the influence of central mass parameters on the characteristics of the transducer. Given that the equivalent circuit is presented in the simplest form, and does not consider the influence of the central bolt, the dependencies shown do not require complex mathematical operations. On the other hand, the bolt extends along the entire structure and is connected mechanically in parallel to the remaining elements in the scheme from Fig. 1. As already noted, most 1D models do not include the bolt impact, or include only a part of it, hence the accuracy of the model in predicting the transducer behaviour is reduced, even in the case of transducers with longer metal endings. The validity and efficacy of the model was verified through the fabrication and characterization of a transducers with various metal parts dimensions. Also, in the proposed transducer model, it is assumed that the circuit elements are ideal, i.e. they do not have losses. Losses can be included if piezoelectric constants and constants of elasticity of the transducer metal parts are in the form of complex numbers, in which the imaginary parts represent losses.

This work can be extended to structural optimization of the whole transducer. The proposed equivalent circuit can be used to obtain the wideband characteristics of transducer in a much more efficient manner than by conventional methods such as the finite element method. The developed structure can be readily extended to an arbitrary number of stacks in the transducer with any number of PZT rings in each stack.

Acknowledgment

This work has been supported by the Ministry of science, technological development and innovation of the Republic of Serbia, contract no. 451-03-47/2023-01/200102.

References

[1] S. Kumar, C. S. Wu, G. K. Padhy, W. Ding, “Application of ultrasonic vibrations in welding and metal processing: A status review,” *Journal of Manufacturing Processes*, vol. 26, pp. 295-322, Apr. 2017.

[2] N. N. Mahamuni, Y. G. Adewuyi, “Advanced oxidation processes (AOPs) involving ultrasound for waste water treatment: A review with emphasis on cost estimation,” *Ultrasonics Sonochemistry*, vol. 17, no.6, pp. 990-1003, Aug. 2010.

[3] Q. Zhang, S. Shi, W. Chen, “An electromechanical coupling model of a longitudinal vibration type piezoelectric ultrasonic transducer,” *Ceramics International*, vol. 41, pp. S638-S644, July 2015.

[4] N. Takayuki, F. Takamichi, E. Masayoshi, T. Shuji, “A large-scan-angle piezoelectric MEMS optical scanner actuated by a Nb-doped PZT thin film,” *Journal of Micromechanics and Microengineering*, vol. 24, no. 1, pp. 015010(1-12), Dec. 2013.

[5] C. Wei, X. Jing, “A comprehensive review on vibration energy harvesting: Modelling and realization,” *Renewable and Sustainable Energy Reviews*, vol. 74, pp. 1-18, July 2017.

[6] F. Boukazouhaa, G. P.-Vittrantb, L. P. T.-H.-Huec, M. Bavencoffec, F. Boubenider, M. Rguitie, M. Lethiecqb, “A comparison of 1D analytical model and 3D Finite Element Analysis with experiments for a Rosen-type piezoelectric transformer,” *Ultrasonics*, vol. 60, pp. 41-50, July 2015.

[7] K. Zhang, D. S. Wang, P. Wang, Y. Q. Du, “Research on the Broadband Dual-Excited Underwater Acoustic Transducer,” In Advanced Engineering Forum. Trans Tech Publications, Ltd. vols. 2–3, pp. 144–147, 2011.

[8] I. Jovanović, D. Mančić, V. Paunović, M. Radmanović, Z. Petrušić, “A Matlab/Simulink Model of Piezoceramic Ring for Transducer Design," Proceedings of the ICEST 2011, Niš, Serbia, vol. 3, pp. 952-955, 2011.

[9] S. Pyo, M. S. Afzal, Y. Lim, S. Lee, Y. Roh, “Design of a Wideband Tonpilz Transducer Comprising Non-Uniform Piezoceramic Stacks with Equivalent Circuits,” *Sensors*, vol. 21, no. 8, p. 2680, 2021.

[10] W. P. Mason, *Electromechanical transducers and wave filters*, Second edition, Van Nostrand, New York, 1948.

[11] D. Mančić, I. Jovanović, M. Radmanović, Z. Petrušić, “Comparison of one-dimensional models of ultrasonic sandwich transducers” – in Serbian, Proceedings of the XXII Noise and Vibration, Niš, Serbia, pp. 119-127, 2010.

[12] I. Jovanović, D. Mančić, “Matlab/Simulink 1D model of longitudinal wave propagation through piezoceramic rings”, Proceedings of the IcETRAN 2021, Bijeljina, Bosnia and Herzegovina, pp. 229-234, 2021.

[13] I. Jovanović, D. Mančić, U. Jovanović, M. Prokić, “A 3D model of new composite ultrasonic transducer”, *Journal of Computational Electronics*, vol. 16, no. 3, pp. 977-986, Sep. 2017.

[14] L. E. Kinsler, A. R. Frey, A. B. Coppens, J. V. Sanders, *Fundamentals of Acoustics*, 4th ed. Wiley, New York, 1999.

[15] *Properties of Piezoelectricity Ceramics*, Technical Publication TP-226, Morgan Electro Ceramics

 ISBN 978-86-7466-970-9